Journal of Systems Engineering and Electronics
Vol. 31, No. 2, April 2020, pp.415 – 431

Methods for predicting the remaining useful life of equipment in consideration of the random failure threshold

WANG Zezhou, CHEN Yunxiang, CAI Zhongyi, GAO Yangjun*, and WANG Lili

Equipment Management & UAV Engineering College, Air Force Engineering University, Xi'an 710051, China

Abstract: The value range of the failure threshold will generate an uncertain influence on the prediction results for the remaining useful life (RUL) of equipment. Most of the existing studies on the RUL prediction assume that the failure threshold is a fixed value, as they have difficulty in reflecting the random variation of the failure threshold. In connection with the inadequacies of the existing research, an in-depth analysis is carried out to study the effect of the random failure threshold (RFT) on the prediction results for the RUL. First, a nonlinear degradation model with unit-to-unit variability and measurement error is established based on the nonlinear Wiener process. Second, the expectation-maximization (EM) algorithm is used to solve the estimated values of the parameters of the prior degradation model, and the Bayesian method is used to iteratively update the posterior distribution of the random coefficients. Then, the effects of three types of RFT constraint conditions on the prediction results for the RUL are analyzed, and the probability density function (PDF) of the RUL is derived. Finally, the degradation data of aero-turbofan engines are used to verify the correctness and advantages of the method.

Keywords: remaining useful life (RUL) prediction, random failure threshold (RFT), nonlinear Wiener process, measurement error, unit-to-unit variability.

DOI: 10.23919/JSEE.2020.000018

1. Introduction

Engineering practice shows that the prognostics and health management (PHM) technology can effectively improve the safety and reliability of the equipment which can also reduce the maintenance and operating costs, and thus, it garners extensive application in aviation, aerospace, medical treatment, electronics, and other high-safety and high-reliability fields [1 – 5].

The core of the PHM technology is to assess the current health status of the equipment and predict its remaining useful life (RUL) through the online monitoring of the changing data on its key performance parameters [6]. Two categories of models are mainly used — the mechanism model and the data-driven model [7 – 10]. However, as the complexity degree of the equipment structure and functions continues to increase, it becomes increasingly difficult to directly build the mechanism model, which in turn restricts the application of the mechanism model. The data-driven model uses the characteristic quantity of the equipment to describe the degradation process, which in turn achieves the prediction of the equipment RUL. This method has numerous advantages, such as a simple principle, good mathematical characteristics, and wide applicability, and it becomes the mainstream method for current studies on the RUL prediction.

The core of the data-driven model is to assume that the degradation process of the equipment can be characterized by its main performance parameters, such as voltage, current, resistance, capacitance, and crack length [11 – 15], and these performance parameters obey specific stochastic processes, such as the inverse Gaussian process, the Gamma process, and the Wiener process [16 – 20]. However, the actual degradation process of the equipment is often not strictly monotonic but has certain nonmonotonic characteristics; for example, a metalized film capacitor may cause the amount of capacitance to increase instead of decrease due to the self-healing mechanism [21 – 24]. Therefore, the inverse Gaussian process, the Gamma process, and other strictly monotonic stochastic processes are unable to accurately reflect the actual degradation characteristics of the equipment. To achieve an accurate description of the nonmonotonic degradation process, the Wiener process, which has nonmonotonic characteristics, is gradually applied to the modeling of degradation processes and obtains good results.

In engineering practice, the working condition, load, and operating environment will change with time, which causes the complexity of the degradation process of the equipment and the difficulty of the traditional Wiener model to meet the accuracy requirements of the RUL pre-

Manuscript received March 13, 2019.
*Corresponding author.
This work was supported by the China Postdoctoral Science Foundation (2017M623415).

diction [25 – 29]. In order to improve the accuracy of the RUL prediction, researchers propose some improved RUL prediction methods with the consideration of nonlinear processes, unit-to-unit variability, and measurement error [30 – 37], which effectively improve the application range of the RUL prediction model based on the Wiener process.

All above studies on the RUL prediction are developed on the basis of an assumption that the failure threshold (FT) is a fixed value. However, due to the differences between different equipments, the random impact of the environment, and other uncertainties, the FT of different equipments will have randomness, such as deformation of spring, drifts of gyroscope, and wear in mechanical parts [38 – 40], which may have an uncertain effect on the RUL prediction. Therefore, it is necessary to further analyze the random FT (RFT). Peng et al. [41] first put forward the concept of an uncertain (random) FT in the degradation modeling process and analyzed the effect of the uncertain (random) FT on the estimation of the equipment reliability. However, this study does not give the specific distribution type of the FT, nor does it derive an analytical expression of the probability density function (PDF) for the RUL. Based on the linear Wiener process, Usynin et al. [42] discussed the effect of the RFT on the estimation of the equipment reliability in a cumulative damage model but still failed to give the specific distribution type of the FT or an analytical expression for the RUL. Huang et al. [43] assumed that the FT is a normal-type random variable and derived an integral expression for the RUL of equipment at different degradation stages with the consideration of the RFT, but their study gave neither a method for estimating the distribution parameters of the RFT nor an analytical expression for the distribution of the RUL. Wei et al. [44] studied the problem of predicting the RUL of the linearly degraded equipment under the condition that the RFT satisfies a normal distribution, but this study failed to take into account the nonnegative requirement of the RFT. Tang et al. [45] first proposed that the RFT should satisfy the constraint condition of $\omega > 0$ and further analyzed the effect of the normal RFT on the prediction of the equipment RUL. However, this study only carries out an analysis in connection with the linear Wiener process, and it is difficult to apply it to the widely existing used nonlinear Wiener process. Moreover, the constraint condition of $\omega > 0$ for the RFT is not strict, and it will increase the uncertainty of the prediction results and decrease the precision of the RUL prediction.

There are still three deficiencies in the existing studies on the RUL prediction in connection with the RFT. First, the research in connection to a nonlinear degradation process has not been launched, which restricts the scope of application of the methodology. Second, a method for estimating the distribution parameters of the RFT has not been put forward, which decreases the completeness of the methodology. Third, the research in connection with the nonnegative constraint for the RFT is still imperfect, which limits the improvements in the prediction precision and accuracy of the methodology. Therefore, in connection with the existing deficiencies in the research related to the RFT, the nonlinear Wiener process is used in this paper for modeling the degradation model, the expectation-maximization (EM) algorithm is used to estimate the degradation model parameters, and online updates are carried out on the model drift coefficient based on the Bayesian principle. Moreover, based on the historical failure data of the equipment, a maximum likelihood method (MLE) is presented to estimate the distribution parameters of the RFT. On this basis, the effect of the RFT on the prediction results of the equipment RUL under three constraint conditions is analyzed.

The main contribution of this paper include: (i) the proposal of a method for estimating the distribution parameters of the RFT based on the MLE; (ii) the derivation of an analytical expression for the distribution function of the corresponding equipment RUL under the three constraint conditions for the RFT of $\omega \in \mathbf{R}$, $\omega > 0$, and $\omega - x_k > 0$, and an analysis of the differences in the three constraint conditions. Through a practical case analysis of aero-turbofan engines, the proposed method is verified as being helpful in the further expansion of the scope of application in the methods for the RUL prediction, improving the precision and accuracy of the RUL prediction. The flow chart for the work in this paper is shown in Fig. 1.

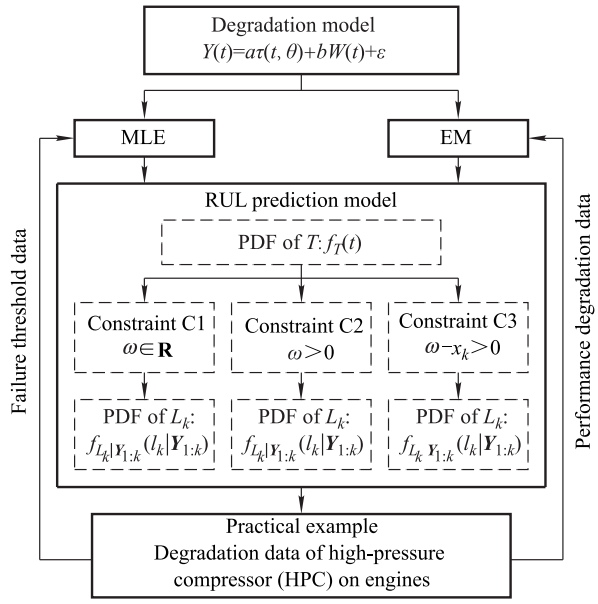

Fig. 1 Flow chart for the work in this paper

The remaining parts of this paper are organized as fol-

lows. Section 2 develops a nonlinear degradation model. Section 3 presents two methods to estimate the parameters of the degradation model and RFT. In Section 4, we update the drift coefficient by using of the Bayesian principle. In Section 5, we separately derive the PDF of the RUL under the three constraints of RFT. A practical example is given to verify the proposed method in Section 6. Section 7 draws the conclusions of this paper.

2. Degradation model

The model of the basic Wiener process for the equipment degradation can be expressed as follows:

$$X(t) = X(0) + at + bW(t) \tag{1}$$

where $X(t)$ represents the amount of equipment performance degradation at time t; $X(0)$ is the amount of equipment performance degradation at the initial time and is generally deemed as $X(0) = 0$; a is the drift coefficient that characterizes the rate at which the equipment performance degrades; $W(t)$ is the standard Brownian motion [$W(t) \sim N(0,t)$]; and b is the diffusion coefficient that characterizes the time-varying uncertainty of the degradation process.

In consideration of the nonlinearity of the degradation process and the individual degradation differences between the same class of the equipment, the following model of the nonlinear Wiener process is given as

$$X(t) = X(0) + a\tau(t,\theta) + bW(t). \tag{2}$$

In (2), to reflect the unit-to-unit variability of the equipment in the degradation process, the drift coefficient a for different equipments is deemed to have randomness and satisfies $a \sim N(\mu_a, \sigma_a^2)$; to reflect the nonlinear features of the degradation process, a nonlinear function of time t, $\tau(t,\theta)$ (θ is the parameter), can be used to describe the nonlinear relationship between the amount of the performance degradation and time.

In consideration of the ubiquitous presence of measurement errors and to reflect the errors in the actual measurement process of the equipment, let the measurement error between the measured value $Y(t)$ and the true value $X(t)$ for the equipment performance degradation be ε, and then the equipment degradation process can be expressed as follows:

$$Y(t) = X(t) + \varepsilon \tag{3}$$

where $\varepsilon \sim N(0, \sigma_\varepsilon^2)$; and the drift coefficient a, the standard Brownian motion $W(t)$, and the measurement error ε are often deemed to be mutually independent.

If ω is used to characterize the FT of the equipment performance degradation, then the life of the equipment can be defined as the time at which the amount of its performance degradation first reaches the FT, that is

$$T = \inf\{t : X(t) \geqslant \omega \big| X(0) < \omega\} \tag{4}$$

where T represents the life of the equipment. In regard to the model of the nonlinear Wiener process described by (2), one can know that its life T approximately obeys an inverse Gaussian distribution, and the PDF is described by (5) [8].

$$f_T(t) \approx \exp\left(-\frac{(\omega - a\tau(t,\theta))^2}{2b^2 t}\right) \cdot \frac{1}{\sqrt{2\pi t^3 b^2}}\left(\omega - \lambda\tau(t,\theta) + at\frac{\mathrm{d}\tau(t,\theta)}{\mathrm{d}t}\right) \tag{5}$$

3. Estimation of parameters

3.1 Estimation of the degradation model parameters

Since the nonlinear Wiener degradation model with the measurement error and the proposed unit-to-unit variability has complexity and implicitness, the EM algorithm is used to estimate the unknown parameters in the degradation model.

Assume that there are performance degradation data for N pieces of the equipment, wherein the monitoring times of the nth equipment are respectively $t_{1,n}, t_{2,n}, \ldots, t_{m_n,n}$, and at the time $t_{i,n}$, the measured amount of the performance degradation for the equipment is $Y_n(t_{i,n})$, and the true amount of the performance degradation for the corresponding equipment is $X_n(t_{i,n})$. Then, $\boldsymbol{Y}_n = [Y_n(t_{1,n}), Y_n(t_{2,n}), \ldots, Y_n(t_{m_n,n})]^{\mathrm{T}}$ represents all monitoring data of the nth equipment, and then $\boldsymbol{Y}_{1:N} = \{\boldsymbol{Y}_1, \boldsymbol{Y}_2, \ldots, \boldsymbol{Y}_N\}$ can be expressed as all performance degradation monitoring data of N pieces of equipment. Let $\Delta Y_n(t_{i,n}) = Y_n(t_{i,n}) - Y_n(t_{i-1,n})$ and $\Delta T_{i,n} = \tau(t_{i,n},\theta) - \tau(t_{i-1,n},\theta)$, then $\Delta\boldsymbol{T}_n = [\Delta T_{1,n}, \Delta T_{2,n}, \ldots, \Delta T_{m_n,n}]^{\mathrm{T}}$, $\Delta\boldsymbol{Y}_n = [\Delta Y_n(t_{1,n}), \Delta Y_n(t_{2,n}), \ldots, \Delta Y_n(t_{m_n,n})]^{\mathrm{T}}$, and $\Delta t_{i,n} = t_{i,n} - t_{i-1,n}$ can be obtained. If the performance degradation process of the equipment is a Wiener process, it is easy to know that $\Delta\boldsymbol{Y}_n$ obeys a multivariate normal distribution, that is, $\Delta\boldsymbol{Y}_n \sim N(\boldsymbol{\mu}_n, \boldsymbol{\Lambda}_n)$, wherein $\boldsymbol{\mu}_n$ is the expectation and $\boldsymbol{\Lambda}_n$ is the covariance matrix.

Assume that a_n is the corresponding drift coefficient of the nth equipment. Then, it can be known based on the properties of a multivariate distribution:

$$\boldsymbol{\mu}_n = a_n\Delta\boldsymbol{T}_n, \tag{6}$$

$$\boldsymbol{\Lambda}_n = b^2\boldsymbol{D}_n + \sigma_\varepsilon^2\boldsymbol{F}_n \tag{7}$$

where a_n is an independent identically distributed normal random variable, and

$$\boldsymbol{D}_n = \mathrm{diag}(\Delta t_{1,n}, \Delta t_{2,n}, \ldots, \Delta t_{m_n,n}), \tag{8}$$

$$\boldsymbol{F}_n=\begin{pmatrix}1&-1&0&\cdots&0\\-1&2&-1&\cdots&\vdots\\0&-1&2&\cdots&0\\\vdots&\vdots&\vdots&\ddots&-1\\0&0&\cdots&-1&2\end{pmatrix}_{m_n\times m_n}. \tag{9}$$

The log-likelihood function of $\boldsymbol{Y}_{1:N}$ is constructed as follows:

$$\begin{aligned}&\ln p(\boldsymbol{Y}_{1:N},a\big|\boldsymbol{\Theta})=\\&-\frac{\ln 2\pi}{2}\sum_{n=1}^{N}m_n-\frac{1}{2}\sum_{n=1}^{N}\ln\big|\boldsymbol{\Lambda}_n\big|-\\&\frac{1}{2}\sum_{n=1}^{N}(\Delta\boldsymbol{Y}_n-\boldsymbol{\mu}_n)^{\mathrm{T}}\boldsymbol{\Lambda}_n^{-1}(\Delta\boldsymbol{Y}_n-\boldsymbol{\mu}_n)-\\&\frac{N}{2}\ln 2\pi-\frac{N}{2}\ln\sigma_a^2-\frac{1}{2\sigma_a^2}\sum_{n=1}^{N}(a_n-\mu_a)^2.\end{aligned} \tag{10}$$

Set $\widehat{\boldsymbol{\Theta}}_{(j)}=(\widehat{\mu}_{a(j)},\widehat{\sigma}^2_{a(j)},\widehat{\theta}_{(j)},\widehat{b}_{(j)},\widehat{\sigma}^2_{\varepsilon(j)})$ to represent the estimated values of the degradation model parameters obtained after the jth step in the iteration, and then the $(j+1)$th step in the iteration process can be divided into the following two steps.

Step 1 Calculate the expectation of the log-likelihood function.

$$\begin{aligned}&L(\boldsymbol{\Theta}\big|\widehat{\boldsymbol{\Theta}}_{(j)})=E_{a|\boldsymbol{Y}_{1:N},\widehat{\boldsymbol{\Theta}}_{(j)}}(\ln p(\boldsymbol{Y}_{1:N},a\big|\widehat{\boldsymbol{\Theta}}_j))=\\&-\frac{\ln 2\pi}{2}\sum_{n=1}^{N}m_n-\frac{N}{2}\ln 2\pi-\\&\frac{N}{2}\ln\widehat{\sigma}^2_{a(j)}-\frac{1}{2}\sum_{n=1}^{N}\ln\big|\boldsymbol{\Lambda}_n(\widehat{b}_{(j)},\widehat{\sigma}^2_{\varepsilon(j)})\big|-\\&\frac{1}{2}\sum_{n=1}^{N}[(\Delta\boldsymbol{Y}_n-E_a(a_n\big|\boldsymbol{Y}_n,\widehat{\boldsymbol{\Theta}}_{(j)})\Delta\boldsymbol{T}_n)^{\mathrm{T}}\boldsymbol{\Lambda}_n(\widehat{b}_{(j)},\widehat{\sigma}^2_{\varepsilon(j)})^{-1}\cdot\\&(\Delta\boldsymbol{Y}_n-E_a(a_n\big|\boldsymbol{Y}_n,\widehat{\boldsymbol{\Theta}}_{(j)})\Delta\boldsymbol{T}_n)+\\&D_a(a_n\big|\boldsymbol{Y}_n,\widehat{\boldsymbol{\Theta}}_{(j)})\Delta\boldsymbol{T}_n^{\mathrm{T}}\boldsymbol{\Lambda}_n(\widehat{b}_{(j)},\widehat{\sigma}^2_{\varepsilon(j)})^{-1}\Delta\boldsymbol{T}_n]-\\&\frac{1}{2\widehat{\sigma}^2_{a(j)}}\sum_{n=1}^{N}[(E_a(a_n\big|\boldsymbol{Y}_n,\widehat{\boldsymbol{\Theta}}_{(j)})-\widehat{\mu}_{a(j)})^2+\\&D_a(a_n\big|\boldsymbol{Y}_n,\widehat{\boldsymbol{\Theta}}_{(j)})]\end{aligned} \tag{11}$$

In a situation in which $\widehat{\boldsymbol{\Theta}}_{(j)}$ and $\boldsymbol{Y}_n$ are known, according to the Bayesian principle, it can be known that $a_n\big|\boldsymbol{Y}_n,\widehat{\boldsymbol{\Theta}}_{(j)}$ obeys the normal distribution. Let $a_n\big|\boldsymbol{Y}_n,\widehat{\boldsymbol{\Theta}}_{(j)}\sim N(E_a(a_n\big|\boldsymbol{Y}_n,\widehat{\boldsymbol{\Theta}}_{(j)}),D_a(a_n\big|\boldsymbol{Y}_n,\widehat{\boldsymbol{\Theta}}_{(j)}))$, and then one can obtain (12) and (13).

$$\begin{aligned}&E_a(a_n\big|\boldsymbol{Y}_n,\widehat{\boldsymbol{\Theta}}_{(j)})=\\&\frac{\widehat{\sigma}^2_{a(j)}\Delta\boldsymbol{T}_n^{\mathrm{T}}\boldsymbol{\Lambda}_{n(j)}(\widehat{b}_{(j)},\widehat{\sigma}^2_{\varepsilon(j)})^{-1}\Delta\boldsymbol{Y}_n+\widehat{\mu}_{a(j)}}{\widehat{\sigma}^2_{a(j)}\Delta\boldsymbol{T}_n^{\mathrm{T}}\boldsymbol{\Lambda}_{n(j)}(\widehat{b}_{(j)},\widehat{\sigma}^2_{\varepsilon(j)})^{-1}\Delta\boldsymbol{T}_n+1}\end{aligned} \tag{12}$$

$$\begin{aligned}&D_a(a_n\big|\boldsymbol{Y}_n,\widehat{\boldsymbol{\Theta}}_{(j)})=\\&\frac{\widehat{\sigma}^2_{a(j)}}{\widehat{\sigma}^2_{a(j)}\Delta\boldsymbol{T}_n^{\mathrm{T}}\boldsymbol{\Lambda}_{n(j)}(\widehat{b}_{(j)},\widehat{\sigma}^2_{\varepsilon(j)})^{-1}\Delta\boldsymbol{T}_n+1}\end{aligned} \tag{13}$$

Step 2 Maximize $L(\boldsymbol{\Theta}\big|\widehat{\boldsymbol{\Theta}}_{(j)})$.

$$\widehat{\boldsymbol{\Theta}}_{(j+1)}=\arg\max_{\boldsymbol{\Theta}}L(\boldsymbol{\Theta}\big|\widehat{\boldsymbol{\Theta}}_{(j)}) \tag{14}$$

Find the partial derivatives of $\widehat{\mu}_{a(j)}$ and $\widehat{\sigma}^2_{a(j)}$ in (11), respectively, and one can get (15) and (16).

$$\frac{\partial L(\boldsymbol{\Theta}\big|\widehat{\boldsymbol{\Theta}}_{(j)})}{\partial\widehat{\mu}_{a(j)}}=\frac{1}{\widehat{\sigma}^2_{a(j)}}\sum_{n=1}^{N}(E_a(a_n\big|\boldsymbol{Y}_n,\widehat{\boldsymbol{\Theta}}_{(j)})-\widehat{\mu}_{a(j)}) \tag{15}$$

$$\begin{aligned}&\frac{\partial L(\boldsymbol{\Theta}\big|\widehat{\boldsymbol{\Theta}}_{(j)})}{\partial\widehat{\sigma}^2_{a(j)}}=-\frac{N}{2\widehat{\sigma}^2_{a(j)}}+\\&\frac{1}{2(\widehat{\sigma}^2_{a(j)})^2}\sum_{n=1}^{N}[(E_a(a_n\big|\boldsymbol{Y}_n,\widehat{\boldsymbol{\Theta}}_{(j)})-\widehat{\mu}_{a(j)})^2+\\&D_a(a_n\big|\boldsymbol{Y}_n,\widehat{\boldsymbol{\Theta}}_{(j)})]\end{aligned} \tag{16}$$

By making (15) and (16) equal zero, one can get (17) and (18).

$$\widehat{\mu}_{a(j+1)}=\frac{1}{N}\sum_{n=1}^{N}E_a(a_n\big|\boldsymbol{Y}_n,\widehat{\boldsymbol{\Theta}}_{(j)}) \tag{17}$$

$$\begin{aligned}&\widehat{\sigma}^2_{a(j+1)}=\frac{1}{N}\sum_{n=1}^{N}[(E_a(a_n\big|\boldsymbol{Y}_n,\widehat{\boldsymbol{\Theta}}_{(j)})-\widehat{\mu}_{a(j+1)})^2+\\&D_a(a_n\big|\boldsymbol{Y}_n,\widehat{\boldsymbol{\Theta}}_{(j)})]\end{aligned} \tag{18}$$

Upon further analysis, it can be known that $\widehat{\mu}_{a(j+1)}$ and $\widehat{\sigma}^2_{a(j+1)}$ exist and are unique; see [46] for specific details of the proof. By bringing (17) and (18) into (11), one can get $\boldsymbol{Y}_{1:N}$ with respect to the profile log-likelihood function for the unknown parameters $\widehat{\theta}_{(j)},\widehat{b}_{(j)},\widehat{\sigma}^2_{\varepsilon(j)}$.

$$\begin{aligned}&L(\boldsymbol{\Theta}\big|\widehat{\boldsymbol{\Theta}}_{(j)},\widehat{\mu}_{a(j+1)},\widehat{\sigma}^2_{a(j+1)})=\\&-\frac{\ln 2\pi}{2}\sum_{n=1}^{N}m_n-\frac{1+\ln 2\pi}{2}N-\\&\frac{N}{2}\ln\widehat{\sigma}^2_{a(j+1)}-\frac{1}{2}\sum_{n=1}^{N}\ln\big|\boldsymbol{\Lambda}_{n(j)}(\widehat{b}_{(j)},\widehat{\sigma}^2_{\varepsilon(j)})\big|-\\&\frac{1}{2}\sum_{n=1}^{N}[(\Delta\boldsymbol{Y}_n-E_a(a_n\big|\boldsymbol{Y}_n,\widehat{\boldsymbol{\Theta}}_{(j)})\Delta\boldsymbol{T}_n)^{\mathrm{T}}\cdot\\&\boldsymbol{\Lambda}_{n(j)}(\widehat{b}_{(j)},\widehat{\sigma}^2_{\varepsilon(j)})^{-1}(\Delta\boldsymbol{Y}_n-E_a(a_n\big|\boldsymbol{Y}_n,\widehat{\boldsymbol{\Theta}}_{(j)})\Delta\boldsymbol{T}_n)+\\&D_a(\lambda_n\big|\boldsymbol{Y}_n,\widehat{\boldsymbol{\Theta}}_{(j)})\Delta\boldsymbol{T}_n^{\mathrm{T}}\boldsymbol{\Lambda}_{n(j)}(\widehat{b}_{(j)},\widehat{\sigma}^2_{\varepsilon(j)})^{-1}\Delta\boldsymbol{T}_n]\end{aligned} \tag{19}$$

By maximizing $L(\boldsymbol{\Theta}\big|\widehat{\boldsymbol{\Theta}}_{(j)},\widehat{\mu}_{a(j+1)},\widehat{\sigma}^2_{a(j+1)})$, one can get $\widehat{\theta}_{(j+1)},\widehat{b}_{(j+1)},\widehat{\sigma}^2_{\varepsilon(j+1)}$. Carry out calculation in Step 1 and Step 2 through iterations until $\|\widehat{\boldsymbol{\Theta}}_{(j+1)}-\widehat{\boldsymbol{\Theta}}_{(j)}\|$ is less than the specified threshold, and then stop. In general, the convergence of the EM algorithm is closely related to the selection of its initial value. To increase the convergence rate of the EM algorithm, the estimated values for the model parameters obtained by MLE can become the initial values of the EM algorithm [47].

3.2 Estimation of the RFT distribution parameters

Assuming that the FT for a given class of the equipment is a random variable that obeys a specific distribution, its PDF can be expressed as $f(\omega)$.

The distribution parameters for the RFT of a single class of the equipment are solved in this paper based on the MLE. Using the normal distribution as an example, assume that the historical degradation data for M equipment of the same class currently exist, and the amounts of the corresponding performance degradation for this type of equipment at the time of failure are $\omega_1,\omega_2,\ldots,\omega_k,\ldots,\omega_M$. Then, the log-likelihood function with respect to the RFT ω can be expressed as follows:

$$\ln L(\omega)=\sum_{k=1}^{M}\ln(f(\omega_k))=$$

$$\sum_{k=1}^{M}\ln\left(\frac{1}{\sqrt{2\pi\sigma_\omega^2}}\exp\left(-\frac{(\omega_k-\mu_\omega)^2}{2\sigma_\omega^2}\right)\right)=$$

$$-\frac{M}{2}\ln(2\pi\sigma_\omega^2)-\sum_{k=1}^{M}\frac{(\omega_k-\mu_\omega)^2}{2\sigma_\omega^2}. \tag{20}$$

The maximization of (20) can obtain the estimated values of the corresponding distribution parameters for the normal RFT as follows:

$$\widehat{\mu}_\omega=\frac{1}{M}\sum_{k=1}^{M}\omega_k, \tag{21}$$

$$\widehat{\sigma}_\omega^2=\frac{1}{M}\sum_{k=1}^{M}(\omega_k-\widehat{\mu}_\omega)^2. \tag{22}$$

4. Online parameter update

To improve the accuracy of the RUL prediction, the equipment performance degradation data obtained in real time are often used to carry out online updates of the equipment degradation model. The specific method is based on the Bayesian principle to carry out updates of the drift coefficient for the degradation model.

To update the drift coefficient for the equipment degradation model under the Bayesian framework, the following Theorem 1 is given in this paper.

Theorem 1 If the priori distribution of the drift coefficient a in the Wiener process obeys a normal distribution, then its posteriori distribution also obeys the normal distribution.

If we let the a priori distribution and a posteriori distribution of a obey $N(\mu_{a_0},\sigma_{a_0}^2)$ and $N(\mu_{a_k},\sigma_{a_k}^2)$, respectively, based on Theorem 1, the update for the drift coefficients can be obtained as shown in (23) and (24).

$$\mu_{a_k}=\frac{\sigma_{a_0}^2\boldsymbol{Y}_k^{\mathrm{T}}\boldsymbol{\Lambda}_k^{-1}\Delta\boldsymbol{T}_k+\mu_{a_0}}{\sigma_{a_0}^2\Delta\boldsymbol{T}_k^{\mathrm{T}}\boldsymbol{\Lambda}_k^{-1}\Delta\boldsymbol{T}_k+1} \tag{23}$$

$$\sigma_{a_k}^2=\frac{\sigma_{a_0}^2}{\sigma_{a_0}^2\Delta\boldsymbol{T}_k^{\mathrm{T}}\boldsymbol{\Lambda}_k^{-1}\Delta\boldsymbol{T}_k+1} \tag{24}$$

The proof of Theorem 1 was given in [47].

5. RUL prediction with RFT

Assume that l_k represents the RUL of the equipment at time t_k, and then $T=t_k+l_k$ can be obtained. Based on the definition of (4) for the equipment life, one can derive the definition for the equipment RUL at time t_k as

$$L=\inf\{l_k:X(t_k+l_k)\geqslant\omega\big|X(0)<\omega\}. \tag{25}$$

Let $\widetilde{X}(l_k)=X(t_k+l_k)-X(t_k)$; if the process of the equipment performance degradation is as shown in (2), then

$$\widetilde{X}(l_k)=a\psi(l_k)+bB(l_k) \tag{26}$$

where $\psi(l_k)=\tau(t_k+l_k,\theta)-\tau(t_k,\theta)$. Without loss of generality, $\widetilde{X}(0)$ is considered equal to zero.

Based on the aforementioned analysis, it can be known that the state of the equipment performance degradation $\widetilde{X}(l_k)$ satisfies the nonlinear Wiener process, and the definition for the equipment RUL can be further transformed by (27).

$$L=\inf\{l_k:\widetilde{X}(l_k)\geqslant\omega-x_k\big|\widetilde{X}(0)<\omega-x_k\} \tag{27}$$

If ω is given, the PDF for the RUL of the nonlinearly degraded equipment can be obtained as follows:

$$f_{L_k\big|\omega,\lambda_k,\boldsymbol{X}_{1:k}}(l_k\big|\omega,\lambda_k,\boldsymbol{X}_{1:k})\approx$$

$$\frac{1}{\sqrt{2\pi b^2l_k^3}}(\omega-x_k-a\beta(l_k))\cdot$$

$$\exp\left(-\frac{(\omega-x_k-a\psi(l_k))^2}{2b^2l_k}\right) \tag{28}$$

where $\beta(l_k)=\psi(l_k)-(\mathrm{d}\psi(l_k)/\mathrm{d}l_k)l_k$.

It can be known from (28) that the PDF of the equipment RUL is closely related to ω. If the randomness of the FT is taken into account, then it will generate an effect on the

randomness of the RUL. It can be found by further analysis that simply taking into account the randomness of the FT is not in line with the reality of the equipment performance degradation. To improve the precision of the RUL prediction, it is also necessary to further consider its nonnegative constraint. To facilitate the analysis, the randomness of the FT will be taken into account, and $\omega \in \mathbf{R}$, $\omega > 0$, and $\omega - x_k > 0$ are recorded as three constraint conditions, C1, C2, and C3, respectively.

In this paper, RFT that satisfies a normal distribution is used as an example for illustration, and the derivation processes of other distribution types are the same as that of the normally distributed RFT.

5.1 RUL prediction under C1

If the equipment degradation process satisfies (2) and there are measurement errors, then $x_k = y_k - \varepsilon \sim N(y_k, \sigma_\varepsilon^2)$ can be obtained. Usually, ω, x_k, and a can be deemed as mutually independent. To derive the PDF of the RUL under C1, Theorem 2 is given in this paper.

Theorem 2 If $D_1 \sim N(\mu_1, \sigma_1^2)$, $D_2 \sim N(\mu_2, \sigma_2^2)$, and $D_3 \sim N(\mu_3, \sigma_3^2)$, any two of D_1, D_2, and D_3 are mutually independent, $E, F \in \mathbf{R}$, and $G \in \mathbf{R}^+$, then

$$E_{D_1}\Bigg[E_{D_2}\Bigg[E_{D_3}\Bigg[(D_1 - D_2 - ED_3)\cdot \exp\left(-\frac{(D_1 - D_2 - FD_3)^2}{2G}\right)\Bigg]\Bigg]\Bigg] = \frac{F^2\sigma_3^2 + G - EF\sigma_3^2}{F^2\sigma_3^2 + \sigma_2^2 + G}\sqrt{\frac{G}{F^2\sigma_3^2 + \sigma_2^2 + \sigma_1^2 + G}}\cdot \left(\frac{(\mu_2 + F\mu_3)\sigma_1^2 + \mu_1(F^2\sigma_3^2 + \sigma_2^2 + G)}{F^2\sigma_3^2 + \sigma_2^2 + \sigma_1^2 + G} - \frac{\mu_2 + E\mu_3}{F^2\sigma_3^2 + G - EF\sigma_3^2}(F^2\sigma_3^2 + \sigma_2^2 + G) + \frac{\mu_2 + F\mu_3}{F^2\sigma_3^2 + G - EF\sigma_3^2}(EF\sigma_3^2 + \sigma_2^2)\right)\cdot \exp\left(-\frac{(\mu_1 - \mu_2 - F\mu_3)^2}{2(F^2\sigma_3^2 + \sigma_2^2 + \sigma_1^2 + G)}\right). \tag{29}$$

Proof To prove Theorem 2, Lemma 1 is given in this paper.

Lemma 1 If $D_1 \sim N(\mu_1, \sigma_1^2)$, $D_2 \sim N(\mu_2, \sigma_2^2)$, D_1 and D_2 are mutually independent, $H, E, F \in \mathbf{R}$, and $G \in \mathbf{R}^+$, then

$$E_{D_1}\left\{E_{D_2}\left[(H - D_1 - ED_2)\cdot \exp\left(-\frac{(H - D_1 - FD_2)^2}{2G}\right)\right]\right\} = \sqrt{\frac{G}{F^2\sigma_2^2 + \sigma_1^2 + G}}\exp\left(-\frac{(H - \mu_1 - F\mu_2)^2}{2(F^2\sigma_2^2 + \sigma_1^2 + G)}\right)\cdot \left(H - \mu_1 - E\mu_2 - \frac{H - \mu_1 - F\mu_2}{F^2\sigma_2^2 + \sigma_1^2 + G}(EF\sigma_2^2 + \sigma_1^2)\right). \tag{30}$$

The proof of Lemma 1 was given in [33].

Lemma 2 If $D \sim N(\mu, \sigma^2)$, $E, F \in \mathbf{R}$ and $G \in \mathbf{R}^+$, then

$$E_D\left[(D - A)\exp\left(-\frac{(D - B)^2}{2C}\right)\right] = \sqrt{\frac{C}{\sigma^2 + C}}\left(\frac{B\sigma^2 + C\mu}{\sigma^2 + C} - A\right)\exp\left(-\frac{(\mu - B)^2}{2(\sigma^2 + C)}\right). \tag{31}$$

The proof of Lemma 2 was given in [32].

Combining the same items for (30), we can get (32) as follows:

$$E_{D_1}\left\{E_{D_2}\left[(H - D_1 - ED_2)\cdot \exp\left(-\frac{(H - D_1 - FD_2)^2}{2G}\right)\right]\right\} = \frac{(F^2\sigma_2^2 - F\sigma_2^2 + G)}{F^2\sigma_2^2 + \sigma_1^2 + G}\sqrt{\frac{G}{F^2\sigma_2^2 + \sigma_1^2 + G}}\cdot \exp\left(-\frac{(H - \mu_1 - F\mu_2)^2}{2(F^2\sigma_2^2 + \sigma_1^2 + G)}\right)\cdot \left(H - \frac{(\mu_1 + E\mu_2)(F^2\sigma_2^2 + \sigma_1^2 + G)}{F^2\sigma_2^2 - EF\sigma_2^2 + G} + \frac{(\mu_1 + F\mu_2)(EF\sigma_2^2 + \sigma_1^2)}{F^2\sigma_2^2 - EF\sigma_2^2 + G}\right). \tag{32}$$

Let

$$D = H, \tag{33}$$

$$A = \frac{(\mu_1 + E\mu_2)(F^2\sigma_2^2 + \sigma_1^2 + G)}{F^2\sigma_2^2 - EF\sigma_2^2 + G} - \frac{(\mu_1 + F\mu_2)(EF\sigma_2^2 + \sigma_1^2)}{F^2\sigma_2^2 - EF\sigma_2^2 + G}, \tag{34}$$

$$B = \mu_1 + F\mu_2, \tag{35}$$

$$C = F^2\sigma_2^2 + \sigma_1^2 + G. \tag{36}$$

By substituting (33), (34), (35) and (36) into (31), the final result of Theorem 2 can be proved directly. □

Based on the total probability, one can get

$$f_{L_k|\boldsymbol{Y}_{1:k}}(l_k|\boldsymbol{Y}_{1:k}) = \int_{-\infty}^{+\infty}\int_{-\infty}^{+\infty}\int_{-\infty}^{+\infty} f_{L_k|\omega,a,\boldsymbol{X}_{1:k}}(l_k|\omega, a, \boldsymbol{X}_{1:k})\cdot p(\omega)p(a|\boldsymbol{Y}_{1:k})p(\boldsymbol{X}_{1:k}|\boldsymbol{Y}_{1:k})\mathrm{d}x_k\mathrm{d}a\mathrm{d}\omega = E_\omega[E_a[E_{x_k}[f_{L_k|\omega,a}, \boldsymbol{X}_{1:k}(l_k|\omega, a, \boldsymbol{X}_{1:k})]]]. \tag{37}$$

Let $\omega = D_1$, $x_k = D_2$, $a = D_3$, $E = \beta(l_k)$, $F = \psi(l_k)$, and $G = b^2 l_k$, and then based on Theorem 2, the PDF of the RUL under RFT conditions can be derived as follows:

$$f_{L_k|\boldsymbol{Y}_{1:k}}(l_k|\boldsymbol{Y}_{1:k}) \approx \frac{\psi(l_k)^2\sigma_{a_k}^2 + b^2 l_k - \beta(l_k)\psi(l_k)\sigma_{a_k}^2}{\psi(l_k)^2\sigma_{a_k}^2 + \sigma_\varepsilon^2 + b^2 l_k} \cdot \sqrt{\frac{1}{2\pi l_k^2(\psi(l_k)^2\sigma_{a_k}^2 + \sigma_\varepsilon^2 + b^2 l_k + \sigma_\omega^2)}} \cdot \exp\left(-\frac{(\mu_\omega - y_k - \psi(l_k)\mu_{a_k})^2}{2(\psi(l_k)^2\sigma_{a_k}^2 + \sigma_\varepsilon^2 + b^2 l_k + \sigma_\omega^2)}\right) \cdot \left(\frac{(y_k + \psi(l_k)\mu_{a_k})\sigma_\omega^2 + \mu_\omega(\psi(l_k)^2\sigma_{a_k}^2 + \sigma_\varepsilon^2 + b^2 l_k)}{\psi(l_k)^2\sigma_{a_k}^2 + \sigma_\varepsilon^2 + b^2 l_k + \sigma_\omega^2} - \frac{(y_k + \beta(l_k)\mu_{a_k})(\psi(l_k)^2\sigma_{a_k}^2 + \sigma_\varepsilon^2 + b^2 l_k)}{\psi(l_k)^2\sigma_{a_k}^2 + b^2 l_k - \beta(l_k)\psi(l_k)\sigma_{a_k}^2} + \frac{(y_k + \psi(l_k)\mu_{a_k})(\beta(l_k)\psi(l_k)\sigma_{a_k}^2 + \sigma_\varepsilon^2)}{\psi(l_k)^2\sigma_{a_k}^2 + b^2 l_k - \beta(l_k)\psi(l_k)\sigma_{a_k}^2}\right). \quad (38)$$

5.2 RUL prediction under C2

It can be known from (4) that the RFT of the equipment should be greater than the initial amount of the performance degradation $X(0)$, that is, $\omega > 0$. To accurately describe the randomness and nonnegativity of ω, the truncated normal distribution is used to characterize the RFT. The specific definition is shown below.

If the RFT ω satisfies $N(\mu_\omega, \sigma_\omega^2)$, and $\omega > 0$, then the RFT obeys a truncated normal distribution and can be expressed as $\omega \sim TN(\mu_\omega, \sigma_\omega^2)$. Its PDF is shown as follows [48]:

$$f(\omega) = \frac{1}{\sqrt{2\pi\sigma_\omega^2}\Phi(\mu_\omega/\sigma_\omega)} \exp\left(-\frac{(\omega - \mu_\omega)^2}{2\sigma_\omega^2}\right). \quad (39)$$

To derive the PDF of the equipment RUL under C2, the PDF of the equipment RUL under the fixed FT conditions is first derived in this paper, and then the PDF of the RUL under RFT conditions is derived. To obtain the PDF of the equipment RUL under the fixed FT conditions, Lemma 3 is given.

Lemma 3 [33] If $D_1 \sim N(\mu_1, \sigma_1^2)$ and $D_2 \sim N(\mu_2, \sigma_2^2)$, where D_1 and D_2 are mutually independent, and $\omega, E, F \in \mathbf{R}$, $G \in \mathbf{R}^+$, then (40) is obtained.

$$E_{D_1}\left\{E_{D_2}\left[(\omega - D_1 - ED_2) \cdot \exp\left(-\frac{(\omega - D_1 - FD_2)^2}{2G}\right)\right] = \sqrt{\frac{G}{F^2\sigma_2^2 + \sigma_1^2 + G}} \exp\left(-\frac{(\omega - \mu_1 - F\mu_2)^2}{2(F^2\sigma_2^2 + \sigma_1^2 + G)}\right) \cdot \left(\omega - \mu_1 - E\mu_2 - \frac{\omega - \mu_1 - F\mu_2}{F^2\sigma_2^2 + \sigma_1^2 + G}(EF\sigma_2^2 + \sigma_1^2)\right) \quad (40)$$

Then, based on the total probability, one can get (41).

$$f_{L_k|\omega,\boldsymbol{Y}_{1:k}}(l_k|\omega, \boldsymbol{Y}_{1:k}) = \int_{-\infty}^{+\infty}\int_{-\infty}^{+\infty} f_{L_k|\omega,a,\boldsymbol{X}_{1:k}}(l_k|\omega, a, \boldsymbol{X}_{1:k}) \cdot p(\boldsymbol{X}_{1:k}|\boldsymbol{Y}_{1:k})p(a|\boldsymbol{Y}_{1:k})\mathrm{d}x_k\mathrm{d}a = E_a\{E_{x_k}[f_{L_k|\omega,a,\boldsymbol{X}_{1:k}}(l_k|\omega, a, \boldsymbol{X}_{1:k})]\} \quad (41)$$

Let $x_k = D_1$, $a = D_2$, $E = \beta(l_k)$, $F = \psi(l_k)$, and $G = b^2 l_k$, and then the PDF of the equipment RUL under the fixed FT conditions can be solved by using Lemma 3 shown as follows:

$$f_{L_k|\omega,\boldsymbol{Y}_{1:k}}(l_k|\omega, \boldsymbol{Y}_{1:k}) \approx \frac{\psi(l_k)^2\sigma_{a_k}^2 + b^2 l_k - \beta(l_k)\psi(l_k)\sigma_{a_k}^2}{\psi(l_k)^2\sigma_{a_k}^2 + b^2 l_k + \sigma_\varepsilon^2} \cdot \sqrt{\frac{1}{2\pi l_k^2(\psi(l_k)^2\sigma_{a_k}^2 + b^2 l_k + \sigma_\varepsilon^2)}} \cdot \exp\left(-\frac{(\omega - (y_k + \mu_{a_k}\psi(l_k)))^2}{2(\psi(l_k)^2\sigma_{a_k}^2 + b^2 l_k + \sigma_\varepsilon^2)}\right) \cdot \left[\omega - \left(\frac{y_k + \mu_{a_k}\beta(l_k)}{\psi(l_k)^2\sigma_{a_k}^2 + b^2 l_k - \beta(l_k)\psi(l_k)\sigma_{a_k}^2} \cdot (\psi(l_k)^2\sigma_{a_k}^2 + b^2 l_k + \sigma_\varepsilon^2) - \frac{y_k + \mu_{a_k}\psi(l_k)}{\psi(l_k)^2\sigma_{a_k}^2 + b^2 l_k - \beta(l_k)\psi(l_k)\sigma_{a_k}^2} \cdot (\beta(l_k)\psi(l_k)\sigma_{a_k}^2 + \sigma_\varepsilon^2)\right)\right]. \quad (42)$$

To obtain the PDF of the equipment RUL under RFT conditions, Theorem 3 is derived.

Theorem 3 If $D \sim TN(\mu, \sigma^2)$, $E, F \in \mathbf{R}$, and $G \in \mathbf{R}^+$, then one can get

$$E_D\left[(D - E)\exp\left(-\frac{(D - F)^2}{2G}\right)\right] = \frac{1}{\sqrt{2\pi\sigma^2}\Phi(\mu/\sigma)} \exp\left(-\frac{(\mu - F)^2}{2(G + \sigma^2)}\right) \cdot \left[\frac{G\sigma^2}{G + \sigma^2}\exp\left(-\frac{(F\sigma^2 + G\mu)^2}{2(G + \sigma^2)G\sigma^2}\right) + \sqrt{\frac{2\pi G\sigma^2}{G + \sigma^2}} \cdot \left(\frac{F\sigma^2 + G\mu}{G + \sigma^2} - E\right)\Phi\left(\frac{F\sigma^2 + G\mu}{\sqrt{(G + \sigma^2)G\sigma^2}}\right)\right]. \quad (43)$$

Proof Let

$$E_D\left[(D-E)\exp\left(-\frac{(D-F)^2}{2G}\right)\right]=$$
$$E_D\left[D\exp\left(-\frac{(D-F)^2}{2G}\right)\right]-$$
$$E_D\left[E\exp\left(-\frac{(D-F)^2}{2G}\right)\right]. \tag{44}$$

If $D\sim TN(\mu,\sigma^2)$, based on the nature of the truncated normal distribution, we can get

$$E_D\left[D\exp\left(-\frac{(D-F)^2}{2G}\right)\right]=\frac{1}{\sqrt{2\pi\sigma^2}\Phi(\mu/\sigma)}\cdot$$
$$\int_0^{+\infty}D\exp\left(-\frac{(D-F)^2}{2G}\right)\exp\left(-\frac{(D-\mu)^2}{2G\sigma^2}\right)\mathrm{d}D=$$
$$\frac{1}{\sqrt{2\pi\sigma^2}\Phi(\mu/\sigma)}\exp\left(-\frac{F^2\sigma^2+\mu^2G}{2\sigma^2G}\right)\cdot$$
$$\exp\left(\frac{(F\sigma^2+\mu G)^2}{2\sigma^2G(\sigma^2+G)}\right)\cdot$$
$$\int_0^{+\infty}D\exp\left(-\frac{\left(D-\dfrac{F\sigma^2+\mu G}{G+\sigma^2}\right)^2}{\dfrac{2G\sigma^2}{G+\sigma^2}}\right)\mathrm{d}D \tag{45}$$

with $A=(F\sigma^2+\mu G)/(G+\sigma^2)$ and $B=G\sigma^2/(G+\sigma^2)$. Then, (45) equals (46).

$$E_D\left[D\exp\left(-\frac{(D-F)^2}{2G}\right)\right]=\frac{1}{\sqrt{2\pi\sigma^2}\Phi(\mu/\sigma)}\cdot$$
$$\exp\left(-\frac{(F-\mu)^2}{2(\sigma^2+G)}\right)\int_0^{+\infty}D\exp\left(-\frac{(D-A)^2}{B}\right)\mathrm{d}D=$$
$$\frac{1}{\sqrt{2\pi\sigma^2}\Phi(\mu/\sigma)}\exp\left(-\frac{(F-\mu)^2}{2(\sigma^2+G)}\right)(I_1+AI_2) \tag{46}$$

I_1 and I_2 can be formulated separately as follows:

$$I_1=\int_0^{+\infty}(D-A)\exp\left(-\frac{(D-A)^2}{B}\right)\mathrm{d}D=$$
$$B\exp\left(-\frac{A^2}{2B}\right), \tag{47}$$
$$I_2=\int_0^{+\infty}\exp\left(-\frac{(D-A)^2}{B}\right)\mathrm{d}D=$$
$$\sqrt{B}\int_{-\frac{A}{\sqrt{B}}}^{+\infty}\exp\left(-\frac{x^2}{2}\right)\mathrm{d}x=\sqrt{2\pi B}\Phi\left(\frac{A}{\sqrt{B}}\right). \tag{48}$$

Based on (48), (49) can be derived easily.

$$E_D\left[D\exp\left(-\frac{(D-F)^2}{2G}\right)\right]=$$
$$\frac{1}{\sqrt{2\pi\sigma^2}\Phi(\mu/\sigma)}\exp\left(-\frac{(F-\mu)^2}{2(\sigma^2+G)}\right)\cdot$$
$$\left[\frac{G\sigma^2}{G+\sigma^2}\exp\left(-\frac{(F\sigma^2+\mu G)^2}{2\sigma^2G(\sigma^2+G)}\right)+\right.$$
$$\left.\frac{F\sigma^2+\mu G}{\sigma^2+G}\sqrt{\frac{2\pi\sigma^2G}{\sigma^2+G}}\Phi\left(\frac{(F\sigma^2+\mu G)}{\sqrt{\sigma^2G(\sigma^2+G)}}\right)\right] \tag{49}$$

By substituting (47) and (48) into (46), (46) can be written as follows:

$$E_D\left[E\exp\left(-\frac{(D-F)^2}{2G}\right)\right]=\frac{E}{\sqrt{2\pi\sigma^2}\Phi(\mu/\sigma)}\cdot$$
$$\int_0^{+\infty}\exp\left(-\frac{(D-F)^2}{2G}\right)\exp\left(-\frac{(D-\mu)^2}{2G\sigma^2}\right)\mathrm{d}D=$$
$$\frac{E}{\sqrt{2\pi\sigma^2}\Phi(\mu/\sigma)}\exp\left(-\frac{(F-\mu)^2}{2(\sigma^2+G)}\right)\cdot$$
$$\int_0^{+\infty}\exp\left(-\frac{(D-A)^2}{2B}\right)\mathrm{d}D=\frac{E}{\sqrt{2\pi\sigma^2}\Phi(\mu/\sigma)}\cdot$$
$$\exp\left(-\frac{(F-\mu)^2}{2(\sigma^2+G)}\right)\sqrt{\frac{2\pi G\sigma^2}{G+\sigma^2}}B\Phi\left(\frac{F\sigma^2+\mu G}{\sqrt{G\sigma^2(G+\sigma^2)}}\right). \tag{50}$$

Then, Theorem 3 can be proved straightforwardly by subtracting (50) from (49). □

Based on the total probability, under the condition in which $\boldsymbol{Y}_{1:k}$ is known, the PDF of the equipment RUL under C2 is derived as follows:

$$f_{L_k|\boldsymbol{Y}_{1:k}}(l_k|\boldsymbol{Y}_{1:k})=$$
$$\int_0^{+\infty}f_{L_k|\omega,\boldsymbol{Y}_{1:k}}(l_k|\omega,\boldsymbol{Y}_{1:k})p(\omega)\mathrm{d}\omega=$$
$$E_\omega[f_{L_k|\omega,\boldsymbol{Y}_{1:k}}(l_k|\omega,\boldsymbol{Y}_{1:k})]. \tag{51}$$

If we let

$$\omega=D, \tag{52}$$
$$G=\psi(l_k)^2\sigma_{a_k}^2+b^2l_k+\sigma_\varepsilon^2, \tag{53}$$
$$F=y_k+\mu_{a_k}\psi(l_k), \tag{54}$$
$$E=\frac{(y_k+\mu_{a_k}\beta(l_k))(\psi(l_k)^2\sigma_{a_k}^2+b^2l_k+\sigma_\varepsilon^2)}{\psi(l_k)^2\sigma_{a_k}^2+b^2l_k-\beta(l_k)\psi(l_k)\sigma_{a_k}^2}-$$
$$\frac{(y_k+\mu_{a_k}\psi(l_k))(\beta(l_k)\psi(l_k)\sigma_{a_k}^2+\sigma_\varepsilon^2)}{\psi(l_k)^2\sigma_{a_k}^2+b^2l_k-\beta(l_k)\psi(l_k)\sigma_{a_k}^2}, \tag{55}$$

and then from (42) and (43), the PDF of the equipment RUL can be derived by using the total probability shown as follows:

$$f_{L_k|\boldsymbol{Y}_{1:k}}(l_k|\boldsymbol{Y}_{1:k})=\frac{\psi(l_k)^2\sigma_{a_k}^2+b^2l_k-\beta(l_k)\psi(l_k)\sigma_{a_k}^2}{\sqrt{\sigma_\omega^2(\psi(l_k)^2\sigma_{a_k}^2+b^2l_k+\sigma_\varepsilon^2)^3}}\frac{1}{2\pi l_k\Phi(\mu_\omega/\sigma_\omega)}\exp\left(-\frac{(\mu_\omega-y_k-\mu_{a_k}\psi(l_k))^2}{2(\psi(l_k)^2\sigma_{a_k}^2+b^2l_k+\sigma_\varepsilon^2+\sigma_\omega^2)}\right)\cdot$$
$$\left[\frac{(\psi(l_k)^2\sigma_{a_k}^2+b^2l_k+\sigma_\varepsilon^2)\sigma_\omega^2}{\psi(l_k)^2\sigma_{a_k}^2+b^2l_k+\sigma_\varepsilon^2+\sigma_\omega^2}\exp\left(-\frac{((y_k+\mu_{a_k}\psi(l_k))\sigma_\omega^2+(\psi(l_k)^2\sigma_{a_k}^2+b^2l_k+\sigma_\varepsilon^2)\mu_\omega)^2}{2(\psi(l_k)^2\sigma_{a_k}^2+b^2l_k+\sigma_\varepsilon^2+\sigma_\omega^2)(\psi(l_k)^2\sigma_{a_k}^2+b^2l_k+\sigma_\varepsilon^2)\sigma_\omega^2}\right)+\right.$$
$$\sqrt{\frac{2\pi(\psi(l_k)^2\sigma_{a_k}^2+b^2l_k+\sigma_\varepsilon^2)\sigma_\omega^2}{\psi(l_k)^2\sigma_{a_k}^2+b^2l_k+\sigma_\varepsilon^2+\sigma_\omega^2}}\left(\frac{(y_k+\mu_{a_k}\psi(l_k))\sigma_\omega^2+(\psi(l_k)^2\sigma_{a_k}^2+b^2l_k+\sigma_\varepsilon^2)\mu_\omega}{\psi(l_k)^2\sigma_{a_k}^2+b^2l_k+\sigma_\varepsilon^2+\sigma_\omega^2}-\right.$$
$$\left.\left.\frac{y_k+\mu_{a_k}\beta(l_k)}{\psi(l_k)^2\sigma_{a_k}^2+b^2l_k-\beta(l_k)\psi(l_k)\sigma_{a_k}^2}(\psi(l_k)^2\sigma_{a_k}^2+b^2l_k+\sigma_\varepsilon^2)+\frac{y_k+\mu_{a_k}\psi(l_k)}{\psi(l_k)^2\sigma_{a_k}^2+b^2l_k-\beta(l_k)\psi(l_k)\sigma_{a_k}^2}(\beta(l_k)\psi(l_k)\sigma_{a_k}^2+\sigma_\varepsilon^2)\right)\cdot\right.$$
$$\left.\Phi\left(\frac{(y_k+\mu_{a_k}\psi(l_k))\sigma_\omega^2+(\psi(l_k)^2\sigma_{a_k}^2+b^2l_k+\sigma_\varepsilon^2)\mu_\omega}{\sqrt{(\psi(l_k)^2\sigma_{a_k}^2+b^2l_k+\sigma_\varepsilon^2+\sigma_\omega^2)(\psi(l_k)^2\sigma_{a_k}^2+b^2l_k+\sigma_\varepsilon^2)\sigma_\omega^2}}\right)\right]. \tag{56}$$

5.3 RUL prediction under C3

It can be known from (27) that the FT of the equipment should be greater than the initial amount of performance degradation $\widetilde{X}(0)$, that is, $\omega-x_k>0$. In general, the amount of performance degradation x_k and the RFT ω can be deemed as mutually independent, and then $\omega-x_k\sim N(\mu_\omega-y_k,\sigma_\omega^2+\sigma_\varepsilon^2)$ can be obtained. In this paper, the truncated normal distribution is used to describe the constraint condition $\omega-x_k>0$, that is, $\omega-x_k\sim TN(\mu_\omega-y_k,\sigma_\omega^2+\sigma_\varepsilon^2)$, and then its PDF is

$$f(\omega-x_k)=\frac{1}{\sqrt{2\pi(\sigma_\omega^2+\sigma_\varepsilon^2)}\Phi((\mu_\omega-y_k)/(\sigma_\omega^2+\sigma_\varepsilon^2))}\cdot\exp\left(-\frac{((\omega-x_k)-(\mu_\omega-y_k))^2}{2(\sigma_\omega^2+\sigma_\varepsilon^2)}\right). \tag{57}$$

Based on the total probability, under the condition in which $\boldsymbol{Y}_{1:k}$ is known, the PDF of the equipment RUL under C3 is derived as follows:

$$f_{L_k|\boldsymbol{Y}_{1:k}}(l_k|\boldsymbol{Y}_{1:k})=\int_0^{+\infty}f_{L_k|\omega-x_k,a}(l_k|\omega-x_k,a)\cdot p(\omega-x_k)p(\lambda_k)\mathrm{d}(\omega-x_k)\mathrm{d}a=\int_0^{+\infty}f_{L_k|\omega,a,\boldsymbol{X}_{1:k}}(l_k|\omega,a,\boldsymbol{X}_{1:k})\cdot p(\omega-x_k)p(a)\mathrm{d}(\omega-x_k)\mathrm{d}a=E_{\omega-x_k}[E_a[f_{L_k|\omega,a,\boldsymbol{X}_{1:k}}(l_k|\omega,a,\boldsymbol{X}_{1:k})]]. \tag{58}$$

To solve the aforementioned expression, Theorem 4 is derived.

Theorem 4 If $D_1\sim N(\mu_1,\sigma_1^2)$ and $D_2\sim N(\mu_2,\sigma_2^2)$, where D_1 and D_2 are mutually independent, and $E,F\in\mathbf{R}$, $G\in\mathbf{R}^+$, then (59) is obtained.

$$E_{D_1}\left[E_{D_2}\left[(D_1-ED_2)\exp\left(-\frac{(D_1-FD_2)^2}{2G}\right)\right]\right]=\frac{F^2\sigma_2^2+G-EF\sigma_2^2}{F^2\sigma_2^2+G}\sqrt{\frac{G}{F^2\sigma_2^2+G}}\cdot$$
$$\frac{1}{\sqrt{2\pi\sigma_1^2}\Phi(\mu_1/\sigma_1)}\exp\left(-\frac{(\mu_1-\mu_2F)^2}{2(F^2\sigma_2^2+G+\sigma_1^2)}\right)\left[\frac{(F^2\sigma_2^2+G)\sigma_1^2}{F^2\sigma_2^2+G+\sigma_1^2}\exp\left(-\frac{(\mu_2F\sigma_1^2+(F^2\sigma_2^2+G)\mu_1)^2}{2(F^2\sigma_2^2+G+\sigma_1^2)(F^2\sigma_2^2+G)\sigma_1^2}\right)+\right.$$
$$\left.\sqrt{\frac{2\pi(F^2\sigma_2^2+G)\sigma_1^2}{F^2\sigma_2^2+G+\sigma_1^2}}\Phi\left(\frac{\mu_2F\sigma_1^2+(F^2\sigma_2^2+G)\mu_1}{\sqrt{(F^2\sigma_2^2+G+\sigma_1^2)(F^2\sigma_2^2+G)\sigma_1^2}}\right)\left(\frac{\mu_2F\sigma_1^2+(F^2\sigma_2^2+G)\mu_1}{F^2\sigma_2^2+G+\sigma_1^2}-\frac{E\mu_2G}{F^2\sigma_2^2+G-EF\sigma_2^2}\right)\right] \tag{59}$$

Proof To prove Theorem 4, Lemma 4 is given.

Lemma 4 If $D_1\sim N(\mu_1,\sigma_1^2)$, $D_2\sim N(\mu_2,\sigma_2^2)$, D_1 and D_2 are mutually independent, $E,F\in\mathbf{R}$, and $G\in\mathbf{R}^+$, then

$$E_{D_2}\left[(D_1-ED_2)\exp\left(-\frac{(D_1-FD_2)^2}{2G}\right)\right]=\sqrt{\frac{G}{F^2\sigma_2^2+G}}\exp\left(-\frac{(D_1-F\mu_2)^2}{2(F^2\sigma_2^2+G)}\right)\cdot\left(D_1-E\mu_2-\frac{D_1-F\mu_2}{F^2\sigma_2^2+G}EF\sigma_2^2\right). \tag{60}$$

The proof of Lemma 4 was given in [32].

Combining the same items for (60), we can get

$$E_{D_2}\left[(D_1-ED_2)\exp\left(-\frac{(D_1-FD_2)^2}{2G}\right)\right]=\sqrt{\frac{G}{F^2\sigma_2^2+G}}\exp\left(-\frac{(D_1-F\mu_2)^2}{2(F^2\sigma_2^2+G)}\right)\cdot\frac{F^2\sigma_2^2+G-EF\sigma_2^2}{F^2\sigma_2^2+G}\left(D_1-\frac{E\mu_2G}{F^2\sigma_2^2+G-EF\sigma_2^2}\right). \quad (61)$$

Then, Theorem 4 can be proved easily by using Theorem 3. □

If we let $\omega-x_k=D_1$, $a=D_2$, $\beta(l_k)=E$, $\psi(l_k)=F$, and $b^2l_k=G$, then (62), the PDF of the equipment RUL, is obtained from (58) and (59).

$$\begin{aligned}f_{L_k|\boldsymbol{Y}_{1:k}}(l_k|\boldsymbol{Y}_{1:k})\approx&\sqrt{\frac{1}{(\psi(l_k)^2\sigma_{a_k}^2+b^2l_k)^3}}\frac{\psi(l_k)^2\sigma_{a_k}^2+b^2l_k-\beta(l_k)\psi(l_k)\sigma_{a_k}^2}{2\pi l_k\sqrt{(\sigma_\omega^2+\sigma_\varepsilon^2)}\Phi((\mu_\omega-y_k)/\sqrt{\sigma_\omega^2+\sigma_\varepsilon^2})}\cdot\\&\exp\left(-\frac{(\mu_\omega-y_k-\mu_{a_k}\psi(l_k))^2}{2(\psi(l_k)^2\sigma_{a_k}^2+b^2l_k+\sigma_\omega^2+\sigma_\varepsilon^2)}\right)\left[\frac{(\psi(l_k)^2\sigma_{a_k}^2+b^2l_k)(\sigma_\omega^2+\sigma_\varepsilon^2)}{\psi(l_k)^2\sigma_{a_k}^2+b^2l_k+\sigma_\omega^2+\sigma_\varepsilon^2}\cdot\right.\\&\exp\left(-\frac{(\mu_{a_k}\psi(l_k)(\sigma_\omega^2+\sigma_\varepsilon^2)+(\psi(l_k)^2\sigma_{a_k}^2+b^2l_k)(\mu_\omega-y_k))^2}{2(\psi(l_k)^2\sigma_{a_k}^2+b^2l_k+\sigma_\omega^2+\sigma_\varepsilon^2)(\psi(l_k)^2\sigma_{a_k}^2+b^2l_k)(\sigma_\omega^2+\sigma_\varepsilon^2)}\right)+\sqrt{\frac{2\pi(\psi(l_k)^2\sigma_{a_k}^2+b^2l_k)(\sigma_\omega^2+\sigma_\varepsilon^2)}{\psi(l_k)^2\sigma_{a_k}^2+b^2l_k+\sigma_\omega^2+\sigma_\varepsilon^2}}\cdot\\&\Phi\left(\frac{\mu_{a_k}\psi(l_k)(\sigma_\omega^2+\sigma_\varepsilon^2)+(\psi(l_k)^2\sigma_{a_k}^2+b^2l_k)(\mu_\omega-y_k)}{\sqrt{(\psi(l_k)^2\sigma_{a_k}^2+b^2l_k+\sigma_\omega^2+\sigma_\varepsilon^2)(\psi(l_k)^2\sigma_{a_k}^2+b^2l_k)(\sigma_\omega^2+\sigma_\varepsilon^2)}}\right)\cdot\\&\left.\left(\frac{\mu_{a_k}\psi(l_k)(\sigma_\omega^2+\sigma_\varepsilon^2)+(\psi(l_k)^2\sigma_{a_k}^2+b^2l_k)(\mu_\omega-y_k)}{\psi(l_k)^2\sigma_{a_k}^2+b^2l_k+\sigma_\omega^2+\sigma_\varepsilon^2}-\frac{\mu_{a_k}b^2l_k\beta(l_k)}{\psi(l_k)^2\sigma_{a_k}^2+b^2l_k-\psi(l_k)\beta(l_k)\sigma_{a_k}^2}\right)\right]\end{aligned} \quad (62)$$

The expectation of the equipment RUL can be expressed as (63) if the randomness of the FT is taken into account.

$$E(l_k|\boldsymbol{Y}_{1:k})=\int_0^{+\infty}l_kf_{L_k|\boldsymbol{Y}_{1:k}}(l_k|\boldsymbol{Y}_{1:k})\mathrm{d}l_k \quad (63)$$

6. Practical case analysis

Analysis and verification are launched based on the commercial modular aero-propulsion system simulation (C-MAPSS) data set provided by the National Aeronautics and Space Administration (NASA), and the 11 aero-turbofan engines in the functional description 001 (FD001) training set are selected as the objects of the analysis [49]. Since the fault mode corresponding to the FD001 data set is the performance degradation of the high-pressure compressor (HPC) on engine, it indicates that the health status of the engine is mainly affected by the performance of the HPC; therefore, the total pressure at the HPC outlet is selected as the main performance indicator for characterizing the health status of the engine. Data on the total pressure at the HPC outlet collected through the pressure sensor are shown in Fig. 2.

It can be known from Fig. 2 that, as the performance of the engine gradually degrades, the total pressure at the HPC outlet of the engine shows a decreasing trend overall. Since the pressure data collected by the sensor have many noise signals, to more accurately reflect the health status level of the engine, the smooth function in MatlAab is used to carry out filter processing on the raw data (set the window width to 30). On this basis, the performance degradation data of the 11 engines are shown in Fig. 3 which can be obtained by subtracting the characteristic state variables at the initial time.

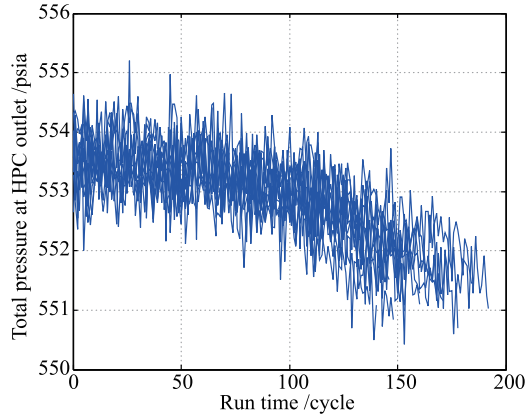

Fig. 2 Data on the total pressure at HPC outlet

6.1 Estimation of the degradation model parameters

It can be known from Fig. 3 that the performance degradation process of the engines exhibits clear nonmonotonicity; therefore, it is appropriate to use the Wiener process to carry out its degradation modeling. To further verify that the performance degradation process of the engines is in line with the Wiener process, the autocorrelation function

method is used to carry out the recognition of the engine degradation process. Based on the basic properties of the Wiener process, the autocorrelation function of the Wiener process shown in (1) can be obtained as follows:

$$\Gamma_{s,t} = E[X(s)X(t)] = \mu^2 st + \sigma^2 \min(s,t). \tag{64}$$

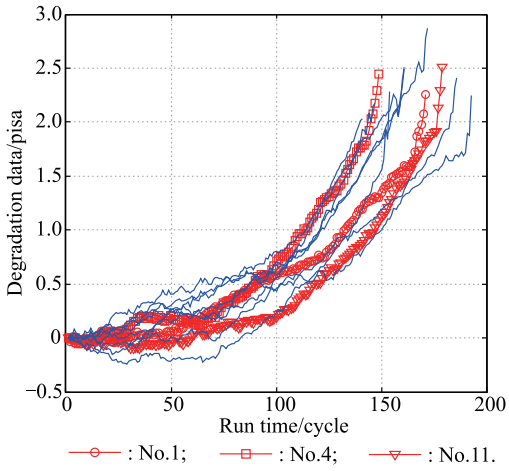

Fig. 3 Degradation data of engines

From (64), the curve of the autocorrelation function for the basic Wiener process can be obtained as shown in Fig. 4.

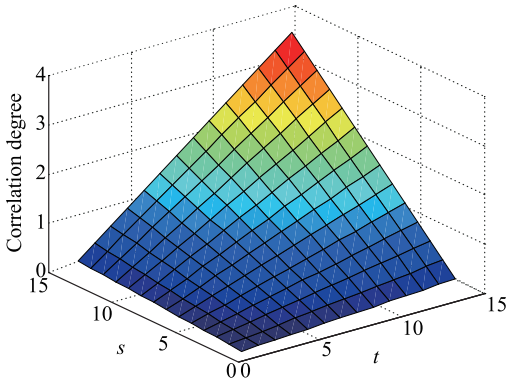

Fig. 4 Autocorrelation function for the basic Wiener process

Since the Wiener process shown in (3) obeys the multivariate normal distribution, it is difficult to obtain the analytical form of its autocorrelation function, and only an estimated value of its moment can be obtained. Assuming that the degradation process of the engines is as shown in (3), then based on the orthogonal invariance of the Wiener process, $\boldsymbol{Y}_n$ can be converted to $\boldsymbol{Z}_n = \boldsymbol{E}\boldsymbol{Y}_n$, where $\boldsymbol{Z}_n$ obeys the normal distribution and $\boldsymbol{E}$ is an orthogonal matrix. The method to calculate $\boldsymbol{E}$ was given in [50].

The moment estimation of the autocorrelation function can be written as follows [50]:

$$\widehat{\Gamma}_{s,t} = \frac{1}{N}\sum_{n=1}^{N}\left(Z_{s,n} - \frac{1}{N}\sum_{n=1}^{N} Z_{s,n}\right)\cdot \left(Z_{t,n} - \frac{1}{N}\sum_{n=1}^{N} Z_{t,n}\right). \tag{65}$$

Based on the above analysis, we can get the moment estimation of the autocorrelation function by using (65) with the degradation data of engines as shown in Fig. 5.

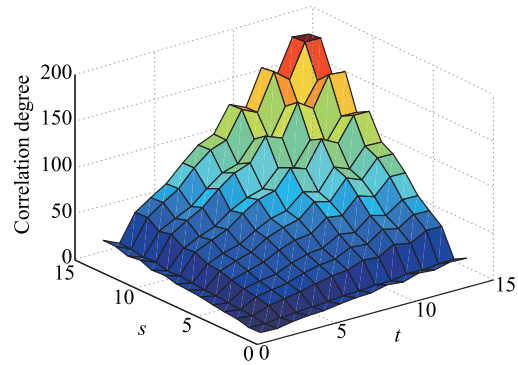

Fig. 5 Autocorrelation function estimation for the degradation data of engines

It can be observed by comparing Fig. 4 and Fig. 5 that the moment estimate of the autocorrelation function is more similar to the autocorrelation function for the basic Wiener process. Therefore, the performance degradation process of the engines can be deemed to satisfy the Wiener process shown in (3).

The historical life data of engines that can be obtained from Fig. 3 are 180, 195, 181, 158, 188, 170, 150, 202, 163, 156, and 179 cycles. In the distribution hypothesis test on the historical life data of all engines, the assumption with an inverse Gaussian distribution is undeniable, which further proves the reasonableness of using the Wiener process to model the performance degradation process of the engines.

It can be determined from Fig. 3 that the performance degradation process of the engines has clear nonlinearity. For this reason, $\tau(t,\theta) = \exp(\theta \cdot t) - 1$ is assumed in this paper. Then, based on the performance degradation data of the engines, the EM algorithm put forward in Section 3.1 is used to carry out the parameter estimation on the engine degradation model, and the estimation results are shown in Fig. 6, wherein $\widehat{\mu}_a = 0.137\ 1$, $\widehat{\sigma}_a^2 = 2.290\ 4\mathrm{e}-5$, $\widehat{\theta} = 0.176\ 7$, $\widehat{b} = 0.030\ 4$, and $\widehat{\sigma}_\varepsilon^2 = 3.980\ 2\mathrm{e}-9$.

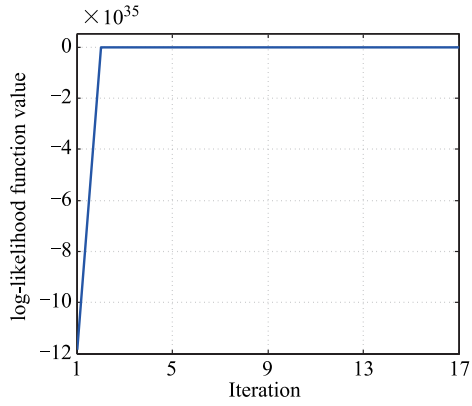

(a) log-likelihood function of $\boldsymbol{Y}_{1:N}$

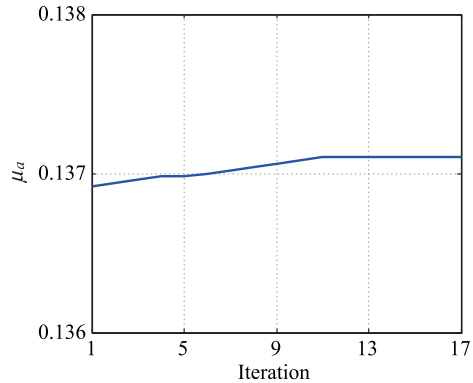

(b) μ_a

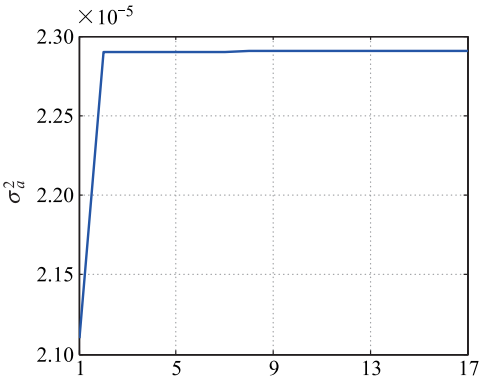

(c) σ_a^2

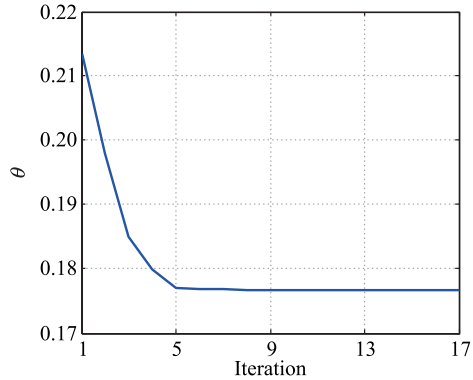

(d) θ

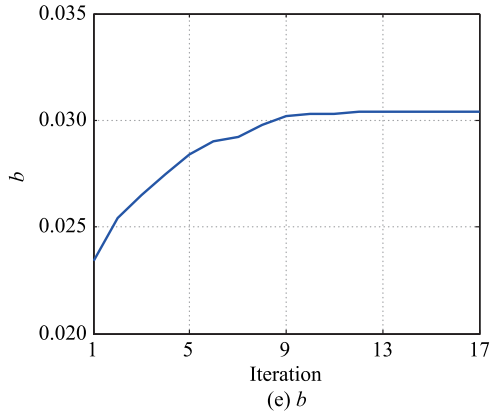

(e) b

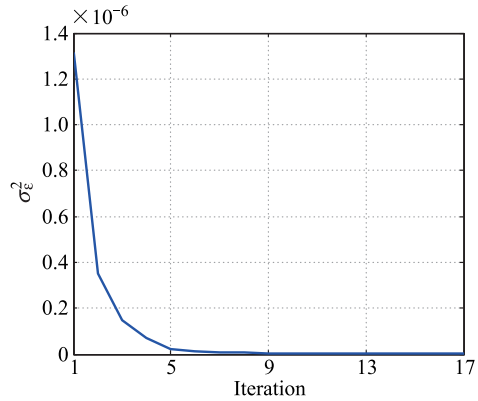

(f) σ_ε^2

Fig. 6 Estimated parameters by EM algorithm

6.2 Estimation of the RFT distribution parameters

The FT is often defined as the amount of performance degradation at the time the equipment fails. The FTs of the 11 engines can be obtained from Fig. 2 and are listed in Table 1.

To determine the specific distribution type of the RFTs, the Kolmogorov-Smirnov (K-S) hypothesis test is carried out on the FTs of engines. The obtained results are listed in Table 2.

Table 1 FTs of engines

Unit	FT	Unit	FT
Item 01	2.253 2	Item 07	2.034 7
Item 02	2.405 8	Item 08	2.247 9
Item 03	2.867 9	Item 09	2.286 8
Item 04	2.441 6	Item 10	2.173 2
Item 05	2.511 1	Item 11	2.506 8
Item 06	2.493 7		

Table 2 K-S test on the distribution of RFTs

Distribution assumption	p	H_0
Normal distribution	0.743 2	0
Weibull distribution	0.509 5	0
Index distribution	0.000 6	1
Poisson distribution	0.000 6	1
Rayleigh distribution	0.003 1	1

It can be determined from Table 2 that it is more reasonable to use the normal distribution to describe the RFT of the engine performance degradation. In this paper, the MLE is used to obtain the distribution parameters of the RFT. For comparison, the results of the least square estimation (LSE) are given in Table 3.

Table 3 Parameter estimation results

Parameter estimation method	$\widehat{\mu}_\omega$	$\widehat{\sigma}_\omega^2$
MLE	2.383 9	0.049 3
LSE1	2.383 9	0.075 8
LSE2	2.383 9	0.062 8
LSE3	2.383 9	0.053 9

In Table 3, LSE1, LSE2, and LSE3 correspond to the three types of empirical functions in [51], i.e., $F(k) = k/(M+1)$, $F(k) = (k-0.3)/(M+0.4)$, and $F(k) = (k-0.5)/M$. We can easily find that the result of LSE depends on the type of the empirical function, which is hard to guarantee the accuracy of the estimation result. However, the MLE does not have the above problem.

To further compare the accuracies of MLE and LSE, the quantile plot of RFTs is given as follows.

Two observations can be drawn from Fig. 7. First, the RFTs are approximately distributed near the datum line, which means the RFTs satisfy the assumption of the normal distribution and it is consistent with the K-S test. Second, the line of the MLE is much closer to the datum line than LSEs, and this indicates that the parameter estimation of the MLE is more accurate than SLEs. In summary, the MLE is used to estimate the distribution parameter of RFTs, which is scientific and reasonable.

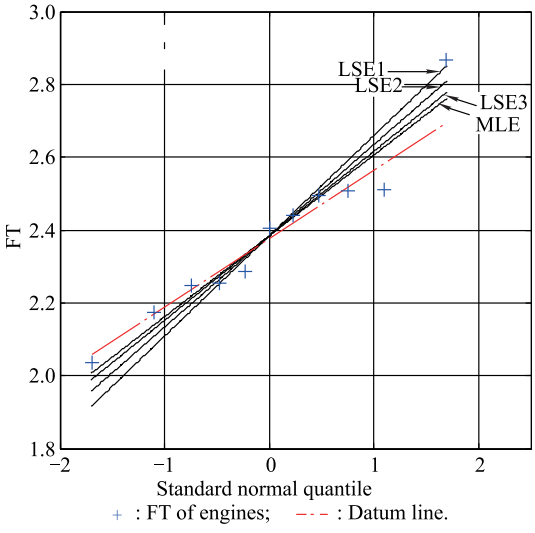

Fig. 7 Quantile plot of RFTs

6.3 RUL prediction

To facilitate the analysis, the method of RUL prediction corresponding to the fixed FT is recorded as M0 in this paper; the method of RUL prediction corresponding to the RFT under constraint C1 is recorded as M1; the method of RUL prediction corresponding to the RFT under constraint C2 is recorded as M2; and the method of RUL prediction corresponding to the RFT under constraint C3 is recorded as M3.

In this paper, we randomly select the 1st, 4th, and 11th engines as the target equipment, and the RUL prediction of each engine is carried out. Based on the degradation data, 95% confidence intervals (CIs) of the prediction RUL at different condition monitoring (CM) times under M0, M1, M2 and M3 are calculated as follows. In the early and middle stages of the degradation process, the CIs under M0, M1, M2 and M3 can completely contain the true RUL of all target equipment, but not all methods are applicable in the late stages of the degradation process. To facilitate the analysis, the CIs in the late stages are shown in Table 4.

Table 4 95% CIs of prediction RUL at different CM times

Engine	CM time	Actual RUL	M0	M1	M2	M3
No.1	155	15	[12.8,22.8]	[9.1,24.0]	[9.5,30.3]	[10.0,29.3]
	160	10	[10.5,19.0]	[6.8,27.8]	[7.1,26.8]	[7.5,25.8]
	165	2	[7.8,15.0]	[4.1,31.3]	[4.3,23.0]	[4.5,22.0]
No.4	120	28	[31.0,49.3]	[21.4,53.85]	[22.4,52.8]	[23.5,51.8]
	130	18	[23.8,39.3]	[14.6,44.3]	[15.2,43.3]	[16.0,42.3]
	140	8	[13.0,25.5]	[4.3,31.8]	[4.5,30.8]	[4.8,29.3]
No.11	155	23	[20.0,30.5]	[12.1,34.0]	[12.6,33.0]	[13.3,32.0]
	165	13	[13.1,21.3]	[5.5,25.0]	[5.7,24.0]	[6.0,23.0]
	175	3	[7.5,13.8]	[1.4,20.0]	[1.4,19.0]	[1.5,16.0]

It can be determined that 95% CIs of the prediction RUL at different CM times under M0 is the narrowest, but it cannot contain the true RUL of all target equipment in each CM time. The CIs of M1, M2 and M3 are wider than that of M0, but they can completely contain the true RUL of the target equipment; the results indicate that the prediction accuracies of M1, M2 and M3 are higher than that of M0. This is mainly because ignoring the randomness of the FT will decrease the uncertainty of the prediction RUL, which in turn causes the CI to be too narrow to contain the true RUL.

The prediction RUL of the 11th engine under M0, M1, M2 and M3 are given as an example to take further analysis in Fig. 8. It can be observed that as the run time increases, the PDF of the RUL predicted by M0, M1, M2 and M3 becomes narrow, indicating that as the status monitoring data increase, the uncertainty of the RUL prediction gradually decreases. In addition, the PDF of the RUL by M0 is more clearly biased to the right than that by M1, M2 and M3, such that the PDF of M0 cannot contain the true RUL at all run times.

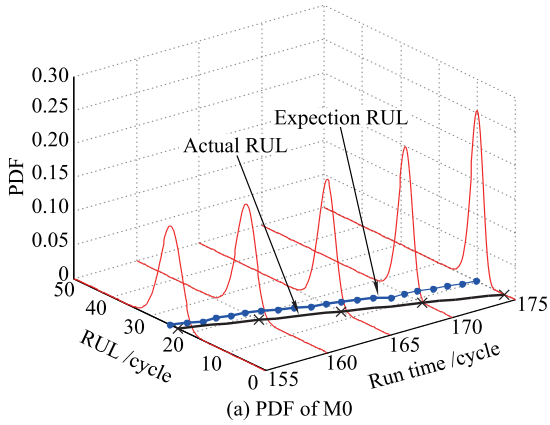

(a) PDF of M0

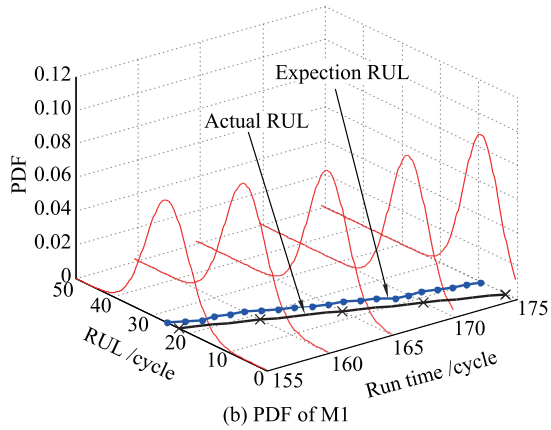

(b) PDF of M1

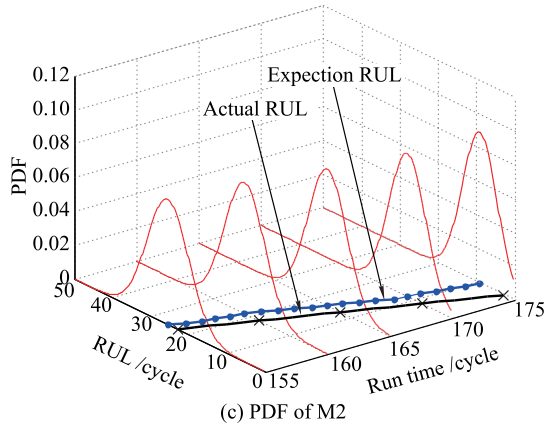

(c) PDF of M2

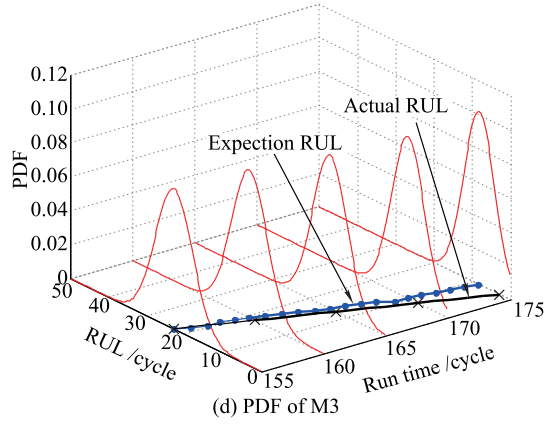

(d) PDF of M3

Fig. 8 Prediction RUL of the 11th engine

It is shown that ignoring the randomness of the FT may lead to an overly optimistic estimation of the RUL, which causes the delayed maintenance and replacement of the engine and may generate a serious effect on flight safety. Therefore, it is extremely necessary to consider the effect of the FT randomness on the RUL prediction process.

To more intuitively reflect the differences among M0, M1, M2 and M3, the PDF of RUL for the 11th engine under M0, M1, M2 and M3 at 172 cycles are shown in Fig. 9.

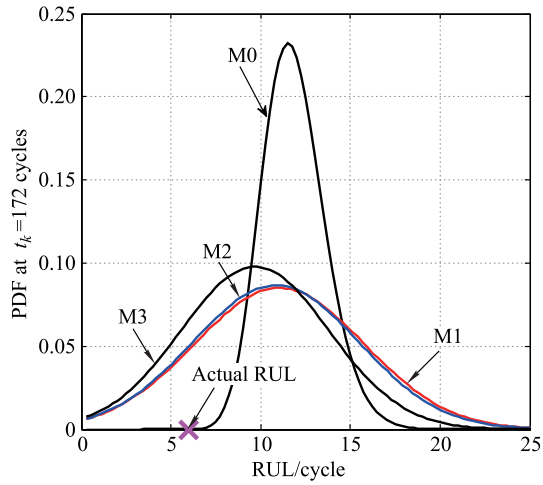

Fig. 9 PDF of RUL at 172 cycles

It can be known from Fig. 9 that, when the 11th engine runs 172 cycles, the PDF of the RUL predictions obtained by M1, M2 and M3 can all contain the true RUL, but the PDF of the RUL corresponding to M3 is clearly narrower than those of M2 and M1, indicating that the precision of the RUL prediction is higher when constraint C3 is taken into account. The main reason for this is that the constraint condition of C3 is stricter than those of C2 and C1, which in turn makes the uncertainty of the RUL prediction smaller, leading to a narrower PDF. In a similar way, since the constraint condition of C2 is stricter than that of C1, it causes the PDF of the RUL corresponding to M2 to be narrower than that of M1. It can be known by a further analysis of Fig. 9 that the PDF under M2 and M1 are almost completely coincident, indicating that there is only a minute gap between M2 and M1. The reason is mainly that the distribution parameter of the RFT, $\widehat{\mu}_\omega >> \widehat{\sigma}_\omega$, causes the truncated normal distribution to approach the normal distribution, resulting in (33) and (43) being approximately equal.

$$\mathrm{MSE} = \int_0^\infty (l_k - T + t_k)^2 f_{L_k|\boldsymbol{Y}_{1:k}}(l_k|\boldsymbol{Y}_{1:k})\mathrm{d}l_k \quad (66)$$

Moreover, we also calculate that the MSEs under M0, M1, M2 and M3 at 172 cycles by using (66) are 37.336 2,

29.924 4, 29.924 3 and 29.688 3, respectively. Since the MSE value is inversely proportional to the prediction accuracy of the method, M3 is proved to be better than M0, M1 and M2. This conclusion is consistent with the analysis results in Fig. 9.

In summary, in the process of the RUL prediction for an engine, taking into account the randomness of the FT and letting it satisfy constraint C3 can effectively improve the prediction precision and accuracy, which in turn provides the decision-making support for the formulation of scientifically reasonable maintenance and engine replacement strategies and helps to improve flight safety and economy.

7. Conclusions

A method for estimating the distribution parameters of the RFT based on MLE is proposed, which has higher estimation accuracy than the LSE.

An in-depth analysis is carried out in connection with the effect of the RFT on the RUL prediction. A practical case analysis shows that the accuracy of the RUL prediction can be effectively improved by taking into account the randomness of the FT.

Further analysis is carried out in connection with three constraint conditions (C1, C2, and C3) for the RFT. A practical case analysis shows that a strict, nonnegative constraint is more helpful in improving the precision of the RUL prediction.

In this paper, a normal distribution is mainly used to describe the randomness of the FT, and a truncated normal distribution is used to reflect the nonnegative constraint condition of the RFT. However, in engineering practice, the RFT may obey other distribution types. Therefore, the RUL prediction in connection with conditions in which the RFT satisfies different distribution types and how to describe the corresponding nonnegative constraint conditions are the focus of future research.

References

[1] BAYBUTT M, MINNELLA C, GINART A E, et al. Improving digital system diagnostics through prognostic and health management (PHM) technology. IEEE Trans. on Instrumentation and Measurement, 2009, 58(2): 255 – 262.

[2] BATZEL T D, SWANSON D C. Prognostic health management of aircraft power generators. IEEE Trans. on Aerospace and Electronic Systems, 2009, 45(04): 473 – 482.

[3] CHOOKAH M, NUHI M, MODARRESN M. A probabilistic physics-of-failure model for prognostic health management of structures subject to pitting and corrosion-fatigue. Reliability Engineering and System Safety, 2011, 96(7): 1601 – 1610.

[4] YAO L, SUN J. The study of prognostic and health management system for smart grid based on wireless sensor networks. Applied Mechanics and Materials, 2015, 719(1): 426 – 430.

[5] HAROON K, AlGAYEM Q, RICHARDSON A M. A housekeeping prognostic health management framework for microfluidic systems. IEEE Trans. on Device and Materials Reliability, 2017, 17(2): 438 – 449.

[6] ANDRES M, GIOVANNI J. Prognostic and health management system for fly-by-wire electro-hydraulic servo actuators for detection and tracking of actuator faults. Procedia CIRP, 2017, 59: 116 – 121.

[7] TSENG K, LIANG J, CHANG W. Regression models using fully discharged voltage and internal resistance for state of health estimation of Lithium-Ion batteries. Energies, 2015, 8(4): 2889 – 2907.

[8] LEI Y, LI N, GONTARZ S, et al. A model-based method for remaining useful life prediction of machinery. IEEE Trans. on Reliability, 2016, 65(3): 1314 – 1326.

[9] WU L, FU X, GUAN Y. Review of the remaining useful life prognostics of vehicle lithium-ion batteries using data-driven methodologies. Applied Sciences, 2016, 6(6): 166 – 176.

[10] LIU D, ZHOU J, PAN D, et al. Lithium-ion battery remaining useful life estimation with an optimized relevance vector machine algorithm with incremental learning. Measurement, 2015, 63(3): 143 – 151.

[11] PHAN T T, HEALEY J T, KENT W R. Microelectronic manufacturing yield, reliability, and failure analysis-prevention of auto-doping-induced threshold voltage shifts. SPIE International Society for Optical Engineering, 1995, 2635: 136 – 144.

[12] URSUTIU D, JONES B K. Low frequency noise used as a lifetime test of LEDs. Journal of Applied Physics, 2004, 96(2): 966 – 969.

[13] PARK C, PADGETT W J. Accelerated degradation models for failure based on geometric Brownian motion and Gamma processes. Lifetime Data Analysis, 2005, 11(4): 511 – 527.

[14] TSENG S T, TANG J, KU I H. Determination of optimal burn-in parameters and residual life for highly reliable products. Naval Research Logistics, 2003, 50(1): 1 – 14.

[15] WANG X, NAIR V. A class of degradation model based on nonhomogeneous Gaussian process. Ann Arbor, America: University of Michigan, 2005.

[16] CAI Z Y, XIANG H C, WANG P, et al. Missile storage lifetime assessment of multivariate degradation modeling under competition failure. Systems Engineering and Electronics, 2018, 40(5): 1183 – 1189. (in Chinese)

[17] LI Z D, ZHANG T. Optimization of inspection and repair of multi-state system under imperfect characteristics. Journal of Beijing University of Aeronautics and Astronautics, 2017, 43(5): 951 – 961. (in Chinese)

[18] PENG C, TSENG S. Mis-specification analysis of linear degradation models. IEEE Trans. on Reliability, 2009, 58(3): 444 – 455.

[19] TANG S J, GUO X, YU C, et al. Accelerated degradation tests modeling based on the nonlinear Wiener process with random effects. Mathematical Problems in Engineering, 2014, 2014(2): 1 – 11.

[20] YE Z, CHEN N, TSUI K L. A Bayesian approach to condition monitoring with imperfect inspections. Quality and Reliability Engineering International, 2015, 31(3): 513 – 522.

[21] MERRITT B T, WHITHAM K. Performance and cost analysis of large capacitor banks using Weibull statistics and MTBF. Proc. of the IEEE International Pulsed Power Conference, 1981.

[22] LARSON D W, MACDOUGALL F W, HARDY P. The impact of high energy density capacitors with metallized electrode in large capacitor banks for nuclear fusion application. Proc. of the 9th IEEE International Pulsed Power Conference, 1993: 735 – 742.

[23] SARIEANT W J, ZIMHELD J, MACDOUGALL F W. Capacitors. IEEE Trans. on Plasma Science, 1998, 26(5): 1368 –

1392.
[24] ZHAO J Y, LIU F. Reliability assessment of the metallized film capacitors from degradation data. Microelectronic Reliability, 2007, 47(2/3): 434 – 436.
[25] CHHIKARA R S, FOLKS J L. The inverse gaussian distribution as a lifetime model. Technometrics, 1977, 19(4): 461 – 468.
[26] DOKSUM K A, HOYLAND A. Models for variable-stress accelerated life testing experiments based on Wiener processes and the inverse Gaussian distribution. Technometrics, 1992, 34(1): 74 – 82.
[27] LIAO H, ELSAYED E A. Reliability inference for field conditions from accelerated degradation testing. Naval Research Logistics, 2006, 53(6): 576 – 587.
[28] WANG X, JIANG P, GUO B, et al. Real-time reliability evaluation for an individual product based on change-point Gamma and Wiener process. Quality and Reliability Engineering International, 2014, 30(4): 513 – 525.
[29] WANG H W, XU T X, WANG W Y. Remaining life prediction based on Wiener processes with ADT prior information. Quality and Reliability Engineering International, 2016, 32(4): 753 – 765.
[30] KAISER K A, GEBRAEEL N Z. Predictive maintenance management using sensor-based degradation models. IEEE Trans. on Systems, Man and Cybernetics, Part A: Systems and Humans, 2009, 39(4): 840 – 849.
[31] WANG X. Wiener processes with random effects for degradation data. Journal of Multivariate Analysis, 2010, 101(2): 340 – 351.
[32] SI X S, WANG W B, HU C H, et al. Remaining useful life estimation based on a nonlinear diffusion degradation process. IEEE Trans. on Reliability, 2012, 61(1): 50 – 67.
[33] TANG S J, GUO X S, YU C Q, et al. Real time remaining useful life prediction based on nonlinear Wiener based degradation processes with measurement errors. Journal of Central South University, 2014, 21(12): 4509 – 4517.
[34] JIANG R. Optimization of alarm threshold and sequential inspection scheme. Reliability Engineering and System Safety, 2010, 95(3): 208 – 215.
[35] SI X S, WANG W B, HU C H, et al. Remaining useful life estimation — a review on the statistical data driven approaches. European Journal of Operational Research, 2011, 213(1): 1 – 14.
[36] YE Z S, WANG Y, TSUI K L, et al. Degradation data analysis using Wiener processes with measurement errors. IEEE Trans. on Reliability, 2013, 62(4): 772 – 780.
[37] WANG Y, YE Z S, TSUI K L. Stochastic evaluation of magnetic head wears in hard disk drives. IEEE Trans. on Magnetics, 2014, 50(5): 1 – 7.
[38] WANG X L, JIANG P, GUO B, et al. Real-time reliability evaluation based on damaged measurement degradation data. Journal of Central South University, 2012, 19(11): 3162 – 3169.
[39] WANG W, CARR M, XU W, et al. A model for residual life prediction based on Brownian motion with an adaptive drift. Microelectronics Reliability, 2011, 51(2): 28 – 293.
[40] WEI M H, CHEN M, ZHOU D. Multi-sensor information based remaining useful life prediction with anticipated performance. IEEE Trans. on Reliability, 2013, 62(1): 183 – 198.
[41] PENG W, DAVID W. Reliability and degradation modeling with random or uncertain failure threshold. Proc. of the Reliability and Maintainability Symposium, 2007: 392 – 397.
[42] USYNIN A, HIENES J W, URMANOV A. Uncertain failure thresholds in cumulative damage models. Proc. of the Reliability and Maintainability Symposium, 2008: 334 – 340.
[43] HUANG J B, KONG D J, CUI L R. Bayesian reliability assessment and degradation modeling with calibrations and RFT. Journal of Shanghai Jiaotong University, 2016, 21(4): 478 – 483.
[44] WEI M, CHEN M, ZHOU D. Multi-sensor information based remaining useful life prediction with anticipated performance. IEEE Trans. on Reliability, 2013, 62(1): 183 – 198.
[45] TANG S J, YU C Q, FENG Y B, et al. Remaining useful life estimation based on Wiener degradation processes with RFT. Journal of Central South University, 2016, 23(9): 2230 – 2241.
[46] EMPSTER A P, LAIRD N M, RUBIN D B. Maximum likelihood from incomplete data via the EM algorithm. Journal of the Royal Statistical Society, 1977, 39 (1): 1 – 38.
[47] TANG S J, YU C Q, WANG X, et al. Remaining useful life prediction of lithium-ion batteries based on the Wiener process with measurement error. Energies, 2014, 7(2): 520 – 547.
[48] GREENE W H. Econometric analysis. New Jersey: Prentice-Hall, 2003.
[49] SAXENA A, KAI G, SIMON D, et al. Damage propagation modeling for aircraft engine run-to-failure simulation. Proc. of the International Conference on Prognostics and Health Management, 2008: 1 – 9.
[50] DAVID R I, RUGGERI F, MICHAEL P W. Bayesian analysis of stochastic process model. New York: Wiley, 2012.
[51] NELSON W. Applied life data analysis. New York: John Wiley & Sons, 1982.

Biographies

WANG Zezhou was born in 1992. He received his B.S. degree in automation and M.S. degree in management science and engineering from Air Force Engineering University, in 2014 and 2016, respectively. Now he is a doctoral student in management science and engineering at Equipment Management & UAV Engineering College, Air Force Engineering University. His research interests include data-driven remaining useful life prediction, reliability assessment and equipment maintenance decision.
E-mail: 350276267@qq.com

CHEN Yunxiang was born in 1962. He received his M.S. degree from Air Force Engineering University in 1989 and Ph.D. degree from Northwestern Polytechnical University in 2005. Now he is a professor of Equipment Management & UAV Engineering College, Air Force Engineering University. His research interests include reliability assessment, material maintenance support, and material development & demonstration.
E-mail: cyx87793@163.com

CAI Zhongyi was born in 1988. He received his B.S. degree in management engineering in 2010, and M.S. and Ph.D. degrees of management science and engineering in 2012 and 2016 from Air Force Engineering University, respectively. Now he is a lecturer of Equipment Management & UAV Engineering College, Air Force Engineering University. His research interests include reliability assessment and remaining life prediction.
E-mail: afeuczy@163.com

GAO Yangjun was born in 1988. He received his B.S. degree in measurement and control technology and instrumentation program from Wuhan University of Technology in 2011 and M.S. degree in control theory and control engineering from Air Force Engineering University in 2014. He is pursuing his Ph.D. degree in systems engineering at Air Force Engineering University. His research interests include the analysis of controllability of complex networks, swarm intelligence algorithm and equipment maintenance decision.
E-mail: greisy2008@gmail.com

WANG Lili was born in 1981. She received her B.S. degree in computer science from Air Force Engineering University in 2003, and M.S. and Ph.D. degrees of management science and engineering from Air Force Engineering University in 2006 and 2009, respectively. Now she is a vice professor of Equipment Management & UAV Engineering College, Air Force Engineering University. Her research interests include reliability design, reliability assessment, and system engineering.
E-mail: 8574886@qq.com